ELSEVIER

Journal of Alloys and Compounds 320 (2001) 126–132

Journal of ALLOYS AND COMPOUNDS

www.elsevier.com/locate/jallcom

Phase relation and thermoelectric properties of the ternary lanthanum chalcogenide system La–A–S (A=Ca, Ba)

S. Katsuyama*, S. Tokuno, M. Ito, K. Majima, H. Nagai

Department of Materials Science and Processing, Graduate School of Engineering, Osaka University, 2-1 Yamadaoka, Suita Osaka 565-0871, Japan

Received 14 December 2000; accepted 15 January 2001

Abstract

The electrical resistivity, Seebeck coefficient and thermal conductivity of $La_{3-x}S_4$, $La_{3-y}A_yS_4$ and $La_2A_zS_3$ (A=Ca, Ba) with the Th_3P_4-type structure have been measured as a function of the composition and temperature. The carrier concentration of these systems can be controlled by the content of *x*, *y* and *z*. With an increase of *x* and *y*, or with a decrease of *z*, the electrical resistivity and Seebeck coefficient increase, while the thermal conductivity decreases. The increase of the electrical resistivity and Seebeck coefficient is due to the decrease of the carrier concentration. For low carrier concentration, the thermal conductivity is mainly governed by the lattice contribution, while for high carrier concentration the carrier contribution dominates. The disordering of the arrangement of the atoms in the crystal lattice accompanied by the substitution or the insertion may affect the phonon scattering, resulting in decreasing the thermal conductivity. The samples with lower carrier concentration show a large figure of merit. $La_{2.27}Ca_{0.73}S_4$ has a maximum figure of merit of 2.9×10^{-4} K^{-1} at about 1000 K.

Keywords: Rare earth compounds; Semiconductors; Electrical transport; Heat conduction; Thermoelectric

1. Introduction

It is known that the rare earth sesquichalcogenide $La_{3-x}S_4$ ($0\leq x\leq 1/3$) has three crystallographic forms, α, β and γ [1]. The low-temperature α phase has an orthorhombic structure with exact stoichiometry of La_2S_3 and exists in the temperature range from room temperature to 1173 K. The β phase has a tetragonal structure and exists from about 1173 to 1573 K. The β phase is also exactly stoichiometric La_2S_3. The α and β phases do not have suitable properties for a thermoelectric material. The high-temperature γ phase forms a cubic defect Th_3P_4-type structure over a composition range La_2S_3 to La_3S_4 [1,2]. The γ phase with Th_3P_4-type structure is well known to have favorable electrical resistivity, Seebeck coefficient, thermal conductivity [2,3,18] and chemical (refractory, low vapor pressure, high melting point [2], etc.) properties which make it suitable as high temperature thermoelectric material. There are 28 lattice sites per unit cell and it is common to write the formula for the unit cell as $4(La_{3-x}\square_xS_4)$, where □ is a lanthanum atom vacancy and $0\leq x\leq 1/3$. For $x=0$, i.e. at the composition La_3S_4, there are no vacancies at the lanthanum site, and for $x=1/3$, i.e. at the composition La_2S_3, 1/9 of the lanthanum sites are vacant. This nonstoichiometric $La_{3-x}S_4$ system has self-doping ability to change continuously from a metallic conductor to an insulator [3,4]. In the case of La_3S_4, three La^{3+} ions contribute nine electrons and four S^{2-} ions accept eight electrons, so that the material shows metallic behavior. In the case of La_2S_3, two La^{3+} ions contribute six electrons and three S^{2-} ions accept six electrons, and so the material is an insulator. Thus, the number of the conduction electrons per unit cell for $La_{3-x}S_4$ changes dependent on *x* and it is denoted by the formula $4(1-3x)$.

It has been reported that the Th_3P_4-type structure is maintained when an alkaline earth metal like Ca, Sr and Ba is substituted for La in γ-La_3S_4 [5–11]. In this substitution system $La_{3-y}A_yS_4$ (A=alkaline earth metal), La can be replaced by alkaline earth metal up to $y=1$. The phase diagram for the ternary La–A–S system is shown in Fig. 1. For $y=0$, i.e. at the composition La_3S_4, the material shows

*Corresponding author.

E-mail address: katsuyama@mat.eng.osaka-u.ac.jp (S. Katsuyama).

0925-8388/01/$ – see front matter
PII: S0925-8388(01)00926-4

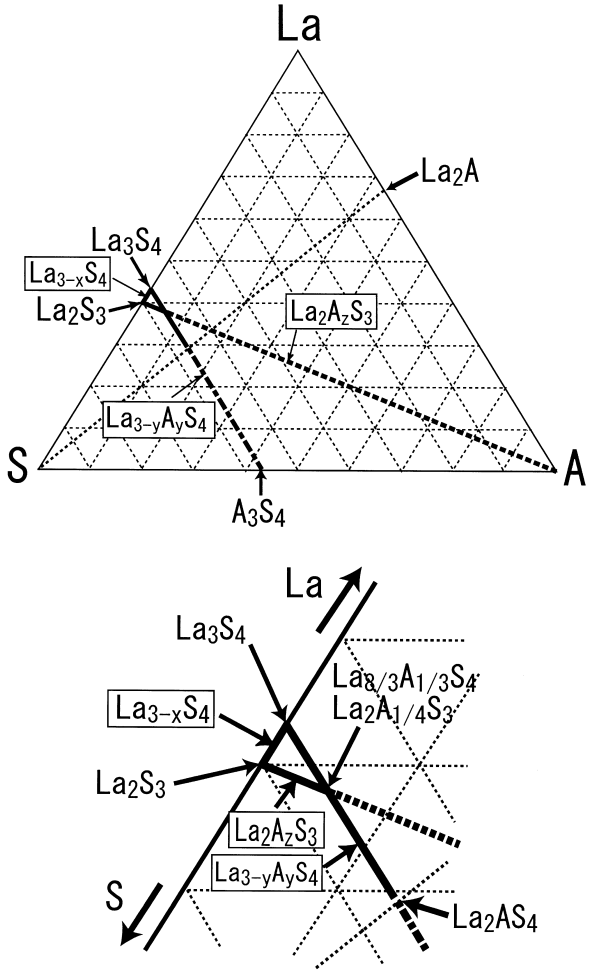

Fig. 1. The phase diagram for the ternary La–A–S (A = alkaline earth metal) system.

metallic behavior as mentioned above. For $y=1$, i.e. at the composition La_2AS_4, two La^{3+} ions contribute six electrons and one divalent A^{2+} ion contributes two electrons, i.e. metal ions contribute eight electrons and four S^{2-} ions accept eight electrons so that the material is an insulator. Thus, in this substitution system, the electrical properties are changed by altering the ratio of lanthanum to alkaline earth metal ions similarly as in the $La_{3-x}S_4$ system. The number of the conduction electrons per unit cell for $La_{3-y}A_yS_4$ is denoted as $4(1-y)$.

We can insert the alkaline earth metal into the lanthanum vacant site of La_2S_3. In this insertion system $La_2A_zS_3$, alkaline earth metal is inserted into lanthanum vacant site up to $z=1/4$. For $z=0$, i.e. at the composition La_2S_3, the material is an insulator as mentioned above. For $z=1/4$, i.e. at the composition $La_2A_{1/4}S_3$, two La^{3+} ions contribute six electrons and 1/4 divalent A^{2+} ion contributes 1/2 electron, i.e. metal ions contribute 13/2 electrons and three S^{2-} ions accept six electrons, and so the material shows metallic behavior. The number of the conduction electrons per unit cell for $La_2A_zS_3$ is denoted as $32/3z$.

The crystallographic mutual relationship among $La_{3-x}S_4$, $La_{3-y}A_yS_4$ and $La_2A_zS_3$ systems and the number of the conduction electrons per unit cell for these three systems are shown in Fig. 2a,b, respectively. The line $La_{3-y}A_yS_4$ in the phase diagram encounters the line of $La_2A_zS_3$ at the composition of $La_{8/3}A_{1/3}S_4$ ($La_2A_{1/4}S_3$), and so $La_{8/3}A_{1/3}S_4$ and $La_2A_{1/4}S_3$ are one and the same.

We have prepared three samples for each system as shown in Table 1. According to the number of the conduction electrons, we can divide these samples into three groups; ($La_{2.76}S_4$, $La_{2.27}A_{0.73}S_4$, $La_2A_{0.1}S_3$), ($La_{2.84}S_4$, $La_{2.53}A_{0.47}S_4$, $La_2A_{0.2}S_3$) and ($La_{2.90}S_4$, $La_{8/3}A_{1/3}S_4$, $La_2A_{1/4}S_3$). Here, $La_{8/3}A_{1/3}S_4$ and $La_2A_{1/4}S_3$ are one and the same, as mentioned above. The samples belonging to the same groups have different chemical compositions, but have almost the same number of conduction electrons. It is interesting to investigate the

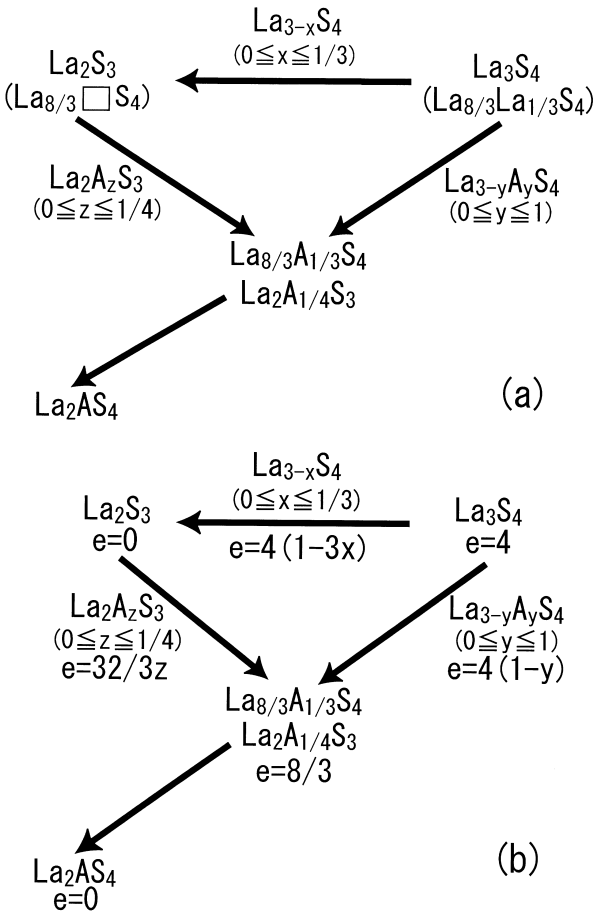

Fig. 2. (a) The phase relationship among $La_{3-x}S_4$, $La_{3-y}A_yS_4$ and $La_2A_zS_3$ systems. (b) The number of the conduction electrons per unit cell volume for $La_{3-x}S_4$, $La_{3-y}A_yS_4$ and $La_2A_zS_3$.

Table 1
The list of the prepared samples and their calculated number of the conduction electrons per unit cell

$La_{3-x}S_4$			$La_{3-y}A_yS_4$			$La_2A_zS_3$		
$La_{2.76}S_4$	$La_{2.84}S_4$	$La_{2.90}S_4$	$La_{2.27}A_{0.73}S_4$	$La_{2.53}A_{0.47}S_4$	$La_{8/3}A_{1/3}S_4$	$La_2A_{0.1}S_3$	$La_2A_{0.2}S_3$	$La_2A_{1/4}S_3$
1.12	2.08	2.8	1.08	2.12	2.67	1.07	2.13	2.67

thermoelectric properties of these samples systematically. Especially, the thermal conductivity is affected by the arrangement of the atoms in the crystal lattice through phonon scattering. The purpose of this study is to measure the Seebeck coefficient, electrical resistivity and thermal conductivity as a function of composition and temperature for $La_{3-x}S_4$, $La_{3-y}A_yS_4$ and $La_2A_zS_3$ (A=Ca, Ba) systems, and to discuss the relationship among the chemical composition, atomic arrangement, carrier concentration and thermoelectric properties of these systems.

2. Experimental

The binary lanthanum sulfide $La_{3-x}S_{4-x}$ ($0<x<1$) was prepared by direct reaction from the elements. The lanthanum metal (Santoku Metal Industry, 99.9 at.% pure) and sulfur (Rare Metallic, 99.999 at.% pure) with the desired composition were evacuated in a quartz ampoule, and were heated at 673 K for 48 h followed by heating at 1273 K for 48 h. After the reaction was completed, the ampoule was opened in an argon-filled glove box and the product was ground into fine powder. For the ternary lanthanum sulfide $La_{3-y}A_yS_4$ (A=Ca, Ba; $0<y\leq 1/3$) and $La_2A_zS_3$ ($0<z\leq 1/4$), the obtained sulfide powder and the commercial CaS (Cerac, 99.99 at.% pure) or BaS (Cerac, 99.9 at.% pure) powder were weighed for the desired compositions and mixed in an argon-filled glove box. The powders were packed in graphite dies and hot-pressed at 1973 K for 3 h at a pressure of 14 MPa under a vacuum of 10^{-3} Pa. The phase identification of the obtained samples was made by X-ray diffraction at room temperature. The Seebeck coefficient (S) and the electrical resistivity (ρ) were measured simultaneously by a standard four-probe dc method under a vacuum of 10^{-3} Pa in a temperature range from room temperature to about 1273 K. The temperature gradient across the length of the sample was about 5 K. Hall measurements were carried out at room temperature by applying an external magnetic field of 1.8 T using a van der Pauw method. The Hall carrier concentration n was obtained using the relationship of $n=1/R_He$, where R_H is the Hall constant and e is the electron charge, assuming a scattering factor equal to 1 and a single carrier model. The thermal diffusion coefficient and the specific heat of the samples were measured by the laser flash method [12] using the thermal constant analyzer (ULVAC TC-7000).

3. Results and discussion

X-ray powder diffraction patterns showed all the finally obtained samples to be single phase and to have the high temperature Th_3P_4-type structure. The lattice parameter versus y in $La_{3-y}A_yS_4$ (A=Ca, Ba) is shown in Fig. 3a together with the lattice parameter for $La_{3-x}S_4$. The lattice parameter for $La_{3-x}S_4$ decreases with increasing x. We can estimate the lattice parameter for La_3S_4 by extrapolating the lattice parameter for $La_{3-x}S_4$ to $x=0$. The estimated value of lattice parameter for La_3S_4, which is denoted with an arrow in the figure, is about 0.8725 nm. The lattice parameter for $La_{3-y}Ca_yS_4$ is smaller than 0.8725 nm and it decreases with increasing y more sharply than in the case of the $La_{3-x}S_4$. On the other hand, the lattice parameter for $La_{3-y}Ba_yS_4$ is much larger than 0.8725 nm and it increases

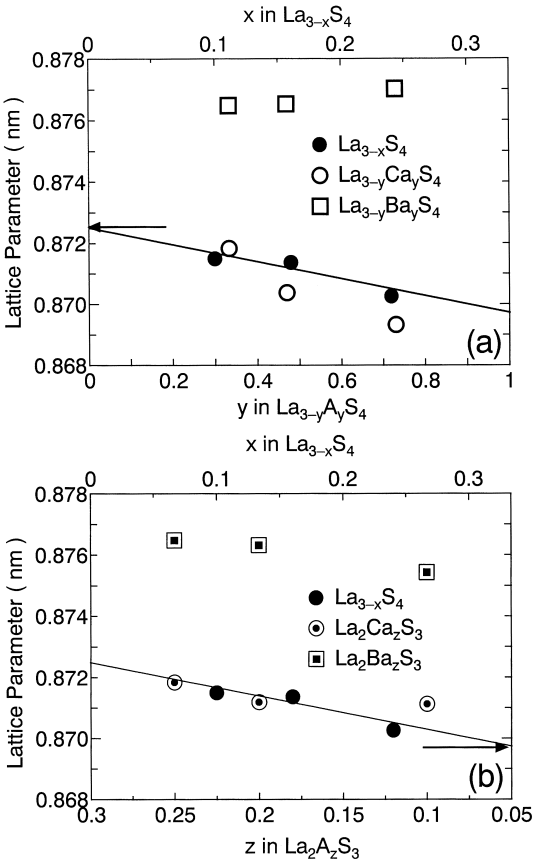

Fig. 3. The content dependence of the lattice parameter for (a) $La_{3-x}S_4$ and $La_{3-y}A_yS_4$, and (b) $La_{3-x}S_4$ and $La_2A_zS_3$ (A=Ca, Ba).

with increasing *y*. These behaviors are in good agreement with the variation in the ionic radii. The radii of La^{3+}, Ca^{2+} and Ba^{2+} are 0.1045, 0.100 and 0.136 nm, respectively [13]. The radius of Ca^{2+} is smaller than that of La^{3+}, while the radius of Ba^{2+} is larger than that of La^{3+}. The change of the lattice parameter is due to the distortion of the lattice accompanied by the replacement of La in La_3S_4 by alkaline earth metal. It is reported that the lattice parameter of the rare earth sesquichalcogenide system is generally sensitive to the ionic size, and it changes linearly with the radius of the rare earth ion [14,15].

The lattice parameter versus *z* in $La_2A_zS_3$ (A=Ca, Ba) is shown in Fig. 3b. The lattice parameter for La_2S_3 can be estimated by extrapolating the lattice parameter for $La_{3-x}S_4$ to $x=1/3$. The estimated value of the lattice parameter for La_2S_3, which is denoted by an arrow in the figure, is about 0.8697 nm. The lattice parameter for $La_2Ca_zS_3$ is larger than 0.8697 nm and it slightly increases with increasing *z*. The lattice parameter for $La_2Ba_zS_3$ is much larger than that for $La_2Ca_zS_3$, to say nothing of that for La_2S_3, and it increases with increasing *z*. Such a change of the lattice parameter for $La_2A_zS_3$ is also due to the distortion of the lattice accompanied by the insertion of alkaline earth metal into the lanthanum site vacancy. The degree of the distortion depends on the difference of the ionic radii. The radius of La^{3+} is slightly larger than that of Ca^{2+}, but is much smaller than that of Ba^{2+}.

Fig. 4 shows the temperature and the composition dependence of the electrical resistivity for $La_{3-x}S_4$, $La_{3-y}Ca_yS_4$ and $La_2Ca_zS_3$. For each composition, the electrical resistivity increases approximately linearly with increasing temperature, i.e. it is metal-like in behavior. The electrical resistivity for $La_{3-x}S_4$ and $La_{3-y}Ca_yS_4$ increases with increasing *x* and *y*, while that for $La_2Ca_zS_3$ decreases with increasing *z*. According to the magnitude of the electrical resistivity, we can divide the samples into three classes: ($La_{2.76}S_4$, $La_{2.27}Ca_{0.73}S_4$, $La_2Ca_{0.1}S_3$), ($La_{2.84}S_4$, $La_{2.53}Ca_{0.47}S_4$, $La_2Ca_{0.2}S_3$) and ($La_{2.90}S_4$, $La_{8/3}Ca_{1/3}S_4(La_2Ca_{1/4}S_3)$). The electrical resistivity for $La_{3-y}Ca_yS_4$ is somewhat larger than that for $La_{3-x}S_4$, but the samples belonging to the same class have almost the same values of electrical resistivity.

Fig. 5 shows the relationship between the calculated values of the carrier concentration and the measured ones for these samples. The calculated values were obtained from the chemical composition and the experimental value of the lattice parameter. The measured values were obtained from the Hall coefficient at room temperature. A straight line with a slope of 45° is drawn in the figure. If the measured value of the carrier concentration agrees with the calculated one, the data point is on the straight line. As shown in the figure, all data points are almost on the straight line and the data points in the same class almost agree. These results indicate that the carrier concentration for these systems can be controlled by altering the chemical composition of the samples and the value of the electrical resistivity for these systems is mainly dominated by the carrier concentration regardless of the chemical composition. It is well known that the transport properties of rare earth chalcogenide with Th_3P_4-type structure are strong functions of the carrier concentration [16,17]. A slight difference in the electrical resistivity among the

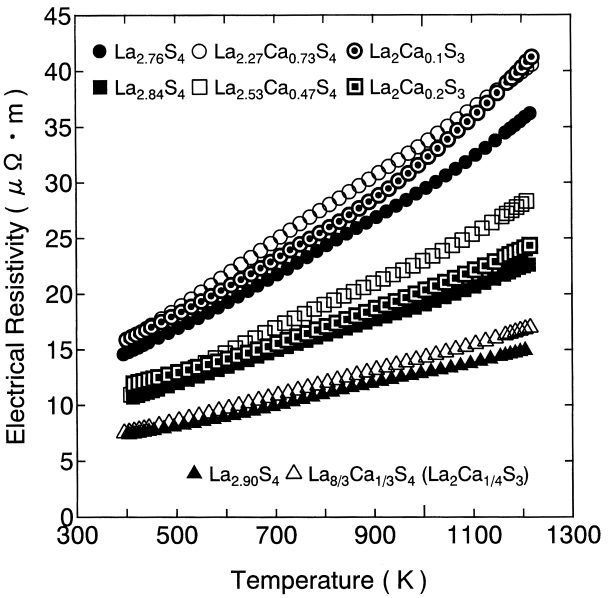

Fig. 4. The temperature and content dependence of the electrical resistivity for $La_{3-x}S_4$, $La_{3-y}Ca_yS_4$ and $La_2Ca_zS_3$.

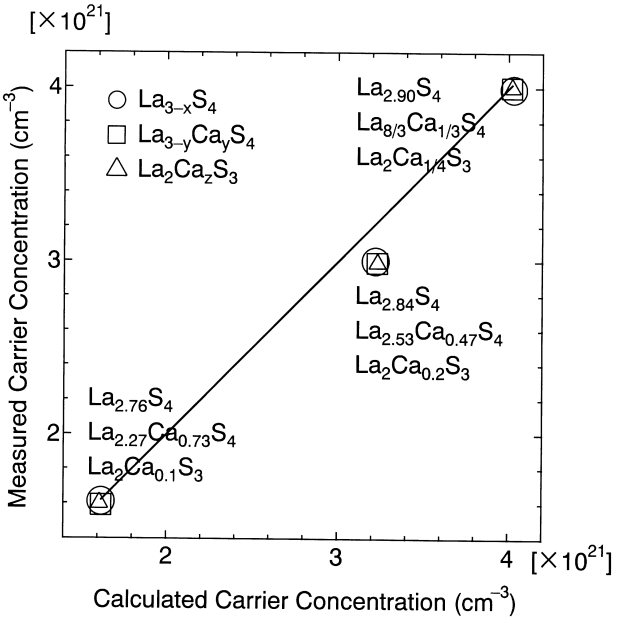

Fig. 5. The measured carrier concentration versus the calculated carrier concentration at room temperature for $La_{3-x}S_4$, $La_{3-y}Ca_yS_4$ and $La_2Ca_zS_3$.

samples belonging to the same class may indicate that the scattering of the carriers is somewhat affected by the atomic arrangement in the crystal lattice. Similar behaviors were also observed in $La_{3-y}Ba_yS_4$ and $La_2Ba_zS_3$ systems.

Fig. 6 shows the results of the Seebeck coefficient of $La_{3-x}S_4$, $La_{3-y}Ca_yS_4$ and $La_2Ca_zS_3$ systems. All Seebeck coefficients are negative, i.e. all these systems are n-type. The absolute value of the Seebeck coefficient increases with increasing temperature. Although it is not so clear, similar behaviors observed in the electrical resistivity are also detected in the Seebeck coefficient. The samples belonging to the same class have almost the same values of the Seebeck coefficients. A similar behaviors were observed in the $La_{3-y}Ba_yS_4$ and $La_2Ba_zS_3$ systems.

The thermal conductivity of the samples is shown in Fig. 7 as a function of the composition and temperature for the $La_{3-x}S_4$, $La_{3-y}Ca_yS_4$ and $La_2Ca_zS_3$ systems. Similar results were obtained in the $La_{3-y}Ba_yS_4$ and $La_2Ba_zS_3$ systems. The thermal conductivity was calculated from the measured thermal diffusivity D, specific heat C_p and density d using the relationship $\kappa = DC_pd$. The thermal conductivity gradually increases with increasing temperature. Similar behaviors are reported by other workers [18]. The thermal conductivity for $La_{3-x}S_4$ and $La_{3-y}Ca_yS_4$ decreases with increasing x and y, while that for $La_2Ca_zS_3$ increases with increasing z. As can be seen from Fig. 5, the carrier concentration n of these systems is denoted as a function of x, y or z; in the case of $La_{3-x}S_4$ and $La_{3-y}Ca_yS_4$, n decreases with increasing x and y, while in the case of $La_2Ca_zS_3$, n increases with increasing z. The decrease of n could lower the thermal conductivity. Furthermore, it is generally assumed that the enhancement of the phonon scattering, which is often induced by the disordered arrangement of the atoms accompanying the substitution or the insertion of the latter, decreases the thermal conductivity. It has been reported that the thermal conductivity of the skutterudite $CoSb_3$ or $IrSb_3$ can be reduced from 9–10 to 3–3.5 W/m per K by forming the solid solution of $Co_{0.88}Ir_{0.12}Sb_3$ or $Co_{0.12}Ir_{0.88}Sb_3$ [19].

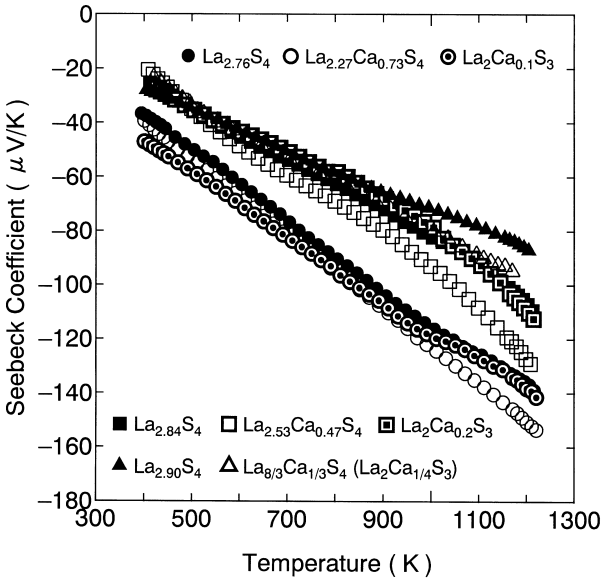

Fig. 6. The temperature and content dependence of the Seebeck coefficient for $La_{3-x}S_4$, $La_{3-y}Ca_yS_4$ and $La_2Ca_zS_3$.

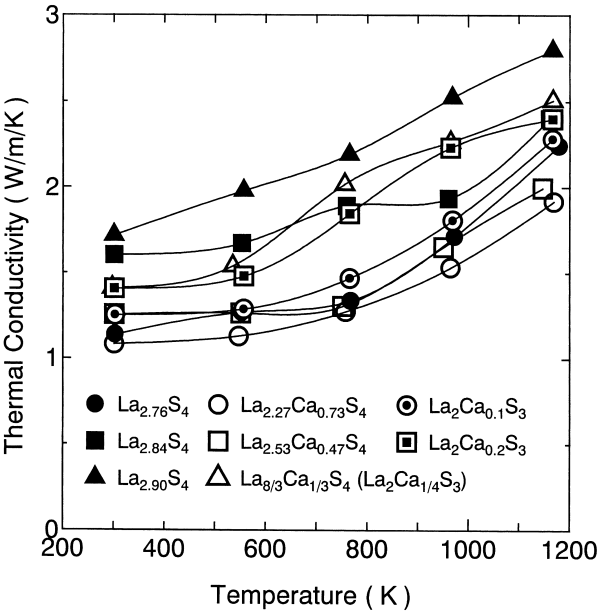

Fig. 7. The temperature and content dependence of the thermal conductivity for $La_{3-x}S_4$, $La_{3-y}Ca_yS_4$ and $La_2Ca_zS_3$.

When a single sign of charge carrier is predominant, the thermal conductivity κ_{total} of the material can be written as

$$\kappa_{total} = \kappa_{car} + \kappa_{ph},$$

where κ_{car} is the carrier contribution and κ_{ph} is the lattice contribution. In order to know which component is responsible for the decrease in the thermal conductivity of these systems, the carrier contribution was calculated using Wiedemann–Franz relationship $\kappa_{car} = L\sigma T$, where L is the Lorenz number, σ is the electrical conductivity and T is the absolute temperature. The Lorenz number was calculated using the reduced Fermi energy, which was estimated from the Seebeck coefficient and the Fermi-Dirac integral. Acoustic-mode phonon scattering was assumed. The lattice contribution κ_{ph} was obtained by subtracting κ_{car} from κ_{total}. The carrier concentration n dependence of κ_{car} and κ_{ph} for $La_{3-x}S_4$, $La_{3-y}Ca_yS_4$ and $La_2Ca_zS_3$ systems at 1173 K is shown in Fig. 8. In the low carrier concentration range, $n < 3\times10^{21}$ cm^{-3}, κ_{ph} is larger than κ_{car}, but in the high carrier concentration range, κ_{car} increases rapidly and κ_{car} becomes larger than κ_{ph} at a concentration of 4×10^{21} cm^{-3}. Thus, the thermal conductivity for these systems is mainly governed by the lattice contribution in the low carrier concentration regime, and in high carrier concentration regime the carrier contribution dominates. These behaviors of the thermal conductivity are similar to those of the LaS_y system reported by Wood et al. [18]. Accord-

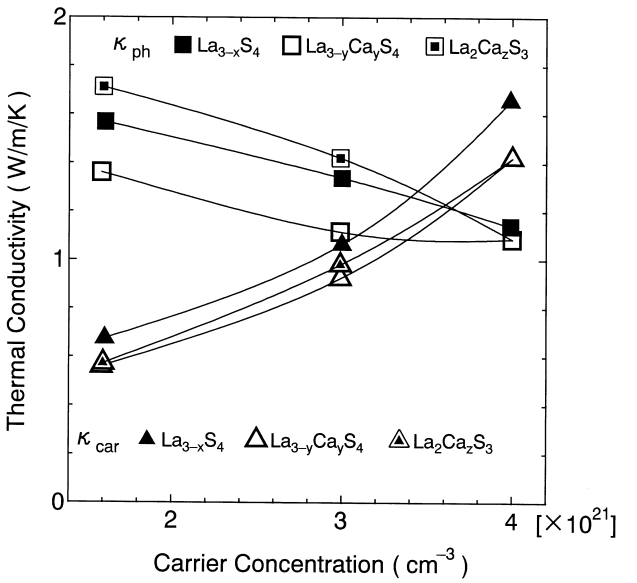

Fig. 8. The carrier concentration dependence of κ_{ph} and κ_{car} at 1173 K for $La_{3-x}S_4$, $La_{3-y}Ca_yS_4$ and $La_2Ca_zS_3$.

ing to these authors, when the carrier concentration falls below 2.5×10^{21} cm^{-3} the lattice contribution is more effective and becomes larger than the carrier contribution. There is almost no difference in κ_{car} among $La_{3-x}S_4$, $La_{3-y}Ca_yS_4$ and $La_2Ca_zS_3$. κ_{ph} decreases with an increase of *n*, i.e. a decrease of *x* and *y* or an increase of *z*. The κ_{ph} value of $La_{3-y}Ca_yS_4$ is somewhat smaller than that of the other two systems. This indicates that the material with larger number of atoms per unit cell has smaller κ_{ph} and

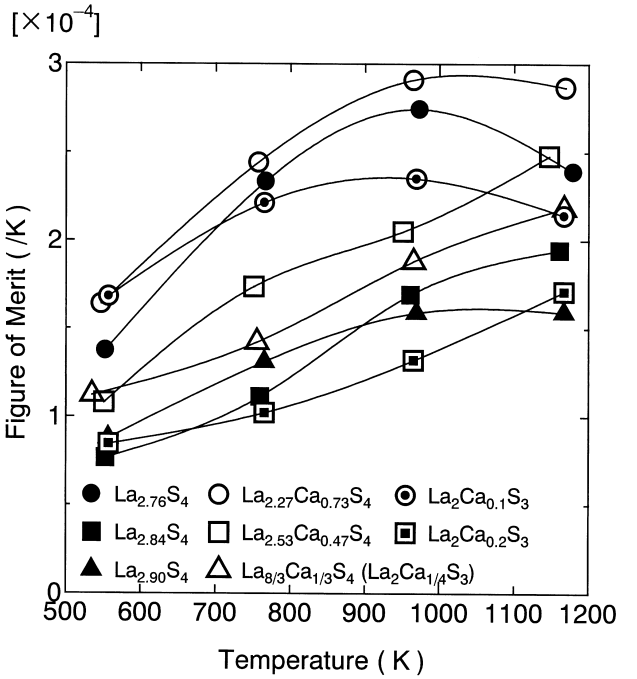

Fig. 9. The temperature and content dependence of the figure of merit for $La_{3-x}S_4$, $La_{3-y}Ca_yS_4$ and $La_2Ca_zS_3$.

the disordering of the arrangement of the atoms accompanying the substitution may affect the phonon scattering, resulting in decreasing κ_{ph}.

The figure of merit Z $(=S^2/(\rho\times\kappa))$ was calculated from the Seebeck coefficient, electrical resistivity and thermal conductivity. Fig. 9 shows the temperature dependence of the figure of merit of $La_{3-x}S_4$, $La_{3-y}Ca_yS_4$ and $La_2Ca_zS_3$ systems. A similar result was obtained in $La_{3-y}Ba_yS_4$ and $La_2Ba_zS_3$. The figure of merit increases with increasing temperature. $La_{2.27}Ca_{0.73}S_4$ has a maximum value of 2.9×10^{-4} K^{-1} at about 1000 K. The figure of merit of $La_{3-y}Ca_yS_4$ is somewhat larger than that of the other two systems. The increase of *Z* in these systems is mainly due to the suppression of the thermal conductivity of the materials.

4. Conclusions

We have prepared three kinds of the rare earth sesquichalcogenide systems, $La_{3-x}S_4$, $La_{3-y}A_yS_4$ and $La_2A_zS_3$ (A=Ca, Ba), and investigated their electrical resistivity, Seebeck coefficient and thermal conductivity to estimate the corresponding figure of merit. All the prepared samples have the high temperature Th_3P_4-type structure. The lattice parameter changes with the composition, which is due to the distortion of the lattice accompanied with the replacement of La by alkaline earth metals or the insertion of alkaline earth metals into the lanthanum site vacancy. The degree of the distortion depends on the difference in ionic radii. The electrical resistivity for $La_{3-x}S_4$ and $La_{3-y}A_yS_4$ increases with increasing *x* and *y*, while that for $La_2A_zS_3$ decreases with increasing *z*. According to the magnitude of the electrical resistivity, the samples can be divided into three classes: ($La_{2.76}S_4$, $La_{2.27}A_{0.73}S_4$, $La_2A_{0.1}S_3$), ($La_{2.84}S_4$, $La_{2.53}A_{0.47}S_4$, $La_2A_{0.2}S_3$) and ($La_{2.90}S_4$, $La_{8/3}A_{1/3}S_4$, $La_2A_{1/4}S_3$). The samples belonging to the same class have almost the same number of the conduction electrons. The Seebeck coefficients of all the samples are negative. Similar behaviors as observed in the electrical resistivity are also detected in the Seebeck coefficient, i.e. the samples belonging to the same class have almost the same value of the Seebeck coefficient. The carrier concentration of these systems can be controlled by altering the chemical composition. In the case of $La_{3-x}S_4$ and $La_{3-y}A_yS_4$, the carrier concentration *n* decreases with increasing *x* and *y*, while in the case of $La_2A_zS_3$, *n* increases with increasing *z*. The electrical resistivity and Seebeck coefficient are mainly dominated by the carrier concentration regardless of the chemical composition of the samples. The thermal conductivity for $La_{3-x}S_4$ and $La_{3-y}A_yS_4$ decreases with increasing *x* and *y*, while that for $La_2A_zS_3$ increases with increasing *z*. The thermal conductivity is mainly governed by the lattice contribution for low carrier concentrations, while for high carrier concentrations the carrier contribu-

tion dominates. The disordered of the arrangement of the atoms in the crystal lattice somewhat affects the lattice contribution of the thermal conductivity.

References

[1] J. Flahaut, in: Handbook on the Physics and Chemistry of Rare Earths, Vol. 4, North-Holland (Physics), Amsterdam, 1979, p. 1.
[2] V.P. Zhuze, V.M. Sergeeva, O.A. Golikova, Sov. Phys. Solid State 11 (1969) 2071.
[3] V.P. Zhuze, O.A. Golikova, V.M. Sergeeva, I.M. Rudnik, Sov. Phys. Solid State 13 (1971) 669.
[4] S.M. Taher, J.B. Gruber, Phys. Rev. B16 (1977) 1624.
[5] J. Flahaut, M. Guittard, M. Patrie, M.P. Pardo, S.M. Golabi, L. Domange, Acta Crystallogr. 19 (1965) 14.
[6] P.D. Provenzano, S.I. Boldish, W.B. White, Mater. Res. Bull. 12 (1977) 939.
[7] M. Sato, G.-Y. Adachi, J. Shiokawa, J. Solid State Chem. 31 (1980) 337.
[8] O. Scheveiw, W.B. White, Mater. Res. Bull. 18 (1983) 1059.
[9] D.L. Chess, C.A. Chess, W.B. White, Mater. Res. Bull. 19 (1984) 1551.
[10] P.J. Walker, R.C.C. Ward, Mater. Res. Bull. 19 (1984) 717.
[11] S. Katsuyama, Y. Tanaka, H. Hashimoto, K. Majima, H. Nagai, J. Appl. Phys. 82 (1997) 5513.
[12] J.W. Vandersande, C. Wood, A. Zoltan, D. Whittenberger, in: Thermal Conductivity, Plenum, New York, 1988, p. 445.
[13] R.D. Shannon, C.T. Prewitt, Acta Crystallogr. Sect. B 25 (1969) 925.
[14] M. Picon, L. Domange, J. Flahaut, M. Guittard, M. Patrie, Bull. Soc. Chim. Fr. 8 (1960) 221.
[15] P.D. Dernier, E. Bucher, L.D. Longinotti, J. Solid State Chem. 15 (1975) 203.
[16] T. Takeshita, K.A. Gschneidner Jr., B.J. Beaudry, J. Appl. Phys. 57 (1985) 4633.
[17] C. Vining, C. Wood, J. Parker, A. Zoltan, L. Danielson, M. Alexander, in: Proceedings of the 7th International Conference on Thermoelectric Energy Conversion, Arlington, TX, 1988, p. 9.
[18] C. Wood, A. Lockwood, J. Parker, A. Zoltan, D. Zoltan, L.R. Danielson, V. Raag, J. Appl. Phys. 58 (1985) 1542.
[19] A. Borshchevsky, J.-P. Fleurial, E. Allevato, T. Caillat, in: Proceedings of the 13th International Conference on Thermoelectrics, Kansas City, MO, 1994, p. 3.